

Modification of Anodized Mg Alloy Surface By Pulse Condition for Biodegradable Material

Y.K. Kim, Y.S. Jang, H.H. Park, J.H. Ji, I.S. Park, T.S. Bae, and M.H. Lee

Abstract—Magnesium is used implant material potentially for non-toxicity to the human body. Due to the excellent bio-compatibility, Mg alloys is applied to implants avoiding removal second surgery. However, it is found commercial magnesium alloys including aluminum has low corrosion resistance, resulting subcutaneous gas bubbles and consequently the approach as permanent bio-materials. Generally, Aluminum is known to pollution substance, and it raises toxicity to nervous system. Therefore especially Mg-35Zn-3Ca alloy is prepared for new biodegradable materials in this study. And the pulsed power is used in constant-current mode of DC power kinds of anodization. Based on the aforementioned study, it examines corrosion resistance and biocompatibility by effect of current and frequency variation. The surface properties and thickness were compared using scanning electronic microscopy. Corrosion resistance was assessed via potentiodynamic polarization and the effect of oxide layer on the body was assessed cell viability. Anodized Mg-35Zn-3Ca alloy has good biocompatibility in vitro by current and frequency variation.

Keywords—Biodegradable material, Mg, anodization, osteoblast cell, pulse power.

I. INTRODUCTION

SINCE the magnesium is the lightest material available metals and excellent specific strength in commercially can obtain a required strength by using a smaller amount than conventional materials [1]. Magnesium has even been suggested for use as an implant metal due to its low weight and inherent biocompatibility [2]. Mg is essential to human metabolism and is toxic-free. Therefore, it is possible to develop a kind of biodegradable magnesium implant, since gradual release of magnesium ion into the human body is acceptable [3]. Commercially available metals, such as AZ91D, AZ31B, WE43 and LAE442 are examined as a degradable Mg material, but the toxicity of aluminum [4] and operation failures due to the formation of hydrogen bubbles during Mg degradation into the body have been reported. A study on the control of the corrosion rate and the improvement of mechanical strength will be required before magnesium can be used as a biomaterial.

Y.K. Kim, H.H. Park, J.H. Ji, T.S. Bae is with the Institute of Oral Bioscience, School of Dentistry, Chonbuk National University, Chonbuk, 561-756, South Korea (phone& fax: 82632704040; e-mail: yk0830@naver.com, raremetals@nate.com, zeast, bts@jbnu.ac.kr).

Y.S.Jang is Dept of Bio-Engineering, North Carolina Agricultural & Technical State University, Greensboro, NC 27411, USA (e-mail: pooh3180@hanmail.net).

H.H. Park is with the BS. COREM Co., Ltd., Chonbuk, 565-902, South Korea (phone& fax: 82632909551; e-mail: raremetals@nate.com).

M.H.Lee, I.S.Park Corresponding Author is with the Institute of Oral Bioscience, School of Dentistry, Chonbuk National University, Chonbuk, 561-756, South Korea (lmh, ilsong@jbnu.ac.kr).

Based on the aforementioned study, this study examined the corrosion resistance and biocompatibility of Mg-35Zn-3Ca alloy to use it as a degradable implant material. Surface treatment is another method to improve the corrosion resistance of Mg alloys. Many protective surface treatments of magnesium alloys, including chemical conversion coating, anodizing, plating and metal coating [5] have been widely studied for improving the corrosion resistance of Mg alloys. Micro-arc oxidation, also call plasma electrolytic, anodic spark deposition or micro-arc discharge oxidizing is a relatively to form ceramic coatings on valve metals in a suitable electrolyte by increasing the voltage to a high stage, usually accompanied by discharge phenomenon and intensive gas evolution [6-9]. Especially plasma anodization is possible with a direct current (DC) or uni/bipolar mode. A pulse current is mainly used in Russia, while in USA; the spark anodization technology is used by applying an alternating current, which can produce a ceramic film with compact and solid adhesion [10]. Therefore, the micro-arc oxidation by frequency and current density variation is applied on new magnesium alloys (Mg-35Zn-3Ca alloy) with the aim of providing protection against corrosion in this study. Also it is valued physical properties and in vitro test on the surface of oxide film for biodegradable magnesium implant.

II. MATERIALS AND METHODS

A. Prepared Material

A Mg-Ca master alloy and Mg-35Zn-3Ca alloy were prepared in this study. For master alloy preparation, Mg (99.93%, Sincere East Co., China) and Ca (99.50%, Junsei Chemical Co., Ltd, Japan) quantities were charged into a Vacuum Arc Remelting Furnace (Ace Vacuum Co., Korea). And it was performed under a current and voltage of 300 A, 12 V while injecting argon gas. Zn was charged into the lower part of melting pot, and Mg was charged into the middle and upper parts of the melting pot. The liquid mixture was poured into an alumina mold to prepare the Mg-35Zn-3Ca alloy. To observe the surface morphology of the casting alloy and to assess the corrosion resistance, a Mg bar with 16 mm in diameter was cut into pieces, 2 mm in thickness, prior to surface treatment. The sectioned plane was sequentially ground using SiC sand paper from # 600 to # 2000.

B. Surface Treatment

For plasma anodization, a platinum plate and sample were connected to the cathode and anode of DC power supply (Kwangduk FA, Korea), respectively using unipolar pulse power. A preliminary test was conducted in an electrolytic solution consisting of 2.0 M sodium hydroxide (NaOH), 0.1 M

sodium phosphate (Na_3PO_4) and 0.1 M sodium silicate (Na_2SiO_3) by regulating the 100–300 mA/cm^2 current density and frequency, as shown in Table I. The start voltage of the pulse was set to 5 V, and the duty cycle of the unipolar pulse power was fixed at 50%, followed by anodization for 3 minute.

C. Analysis of Morphology

The morphological microstructure of the sample surface and cross section for film thickness was observed by SEM (JSM-6400, JEOL, Japan). The surface roughness was measured 5 times using a roughness detector (Surftest SV-3000, Mitutoyo, Japan) to obtain the mean value. After calculating the centerline average roughness (R_a) and maximum height roughness (R_y), the sample group with the densest microstructure of the anodized oxide layer and the most homogenous surface morphology was selected, and then used for biological tests.

TABLE I
VARIATION OF THE TREATMENT CONDITION

Group	Current (mA/cm^2)	Frequency (Hz)	Time (min)
A	100	50	3
B	100	160	
C	200	50	
D	200	160	
E	300	50	
F	300	160	

D. Corrosion Test

To examine the corrosion of the anodized oxide layer, potentiodynamic polarization was conducted using Potentiostatic / Galvanostatic 2273 (AMETEK, USA) to measure the corrosion potential and current density. A Ag/AgCl electrode, platinum electrode, and the sample were connected to the reference electrode, counter electrode and working electrode, respectively. 0.185 g/l calcium chloride dihydrate, 0.09767 g/l magnesium sulfate and 0.350 g/l sodium hydrogen carbonate were added to Hanks Balanced Salt Solution (H2387, Sigma Chemical Co, USA) to prepare the simulated body fluid used as an electrolytic solution. The test was carried out at a scanning rate of 3 $\text{mV}\cdot\text{s}^{-1}$ and room temperature. Table III lists the composition of the SBF.

TABLE II
REAGENT COMPOSITION OF HANK'S SOLUTION

Components	Value (g/L)
Potassium Chloride	0.4
Potassium Phosphate Monobasic [anhydrous]	0.06
Sodium Chloride	8.0
Sodium Phosphate Dibasic[anhydrous]	0.04788
D-Glucose	1.0
Phenol red Na	0.011

E. In vitro Test

Marrow cells (MC3T3) collected from cranium of neogenesis mice. Samples of size $10\times 10\times 2\text{mm}^3$ were cut and immersed in 1mL (1% antibiotic and 10% FBS(Fetal Bovine Serum) including α -MEM(Gibco Co, USA))during 2 days for soaking out. 1% antibiotic and 10% FBS (Fetal Bovine Serum) were chose for culture medium. According to ISO 10993-5:1999[11], extraction was carried out in an extraction medium with a ratio of α -MEM medium: sample weight percent = 9:1 under the condition of a humidified atmosphere with 5% CO_2 at 37°C for 72 hours. A-MEM medium was used as the negative control, whereas α -MEM medium containing 10% dimethyl sulfoxide (DMSO, Duksan pure chemical Co., Ltd. Korea) was used as the positive control. The prepared 1mL culture solution containing of extracted sample were placed on medium cell amount of 5×10^4 cells/well. And then it grows cells during 2 days in 5% CO_2 incubator. Incubation was carried out at 37°C in an atmosphere containing 5 vol. % CO_2 .

The fixing fluids were used by 3% Formaldehyde, 0.2% Glutaraldehyde and PBS, and 0.3% Crystalviolet was used for staining. The cells were fixed and stained prior to morphological analysis by stereoscopic microscope (Leica microsystem DE/EZ 4).

III. RESULTS AND DISCUSSION

Fig. 1 presents SEM images obtained from anodization under a range of conditions for 3 min. A current of 100–300 mA/cm^2 and two frequencies of 50 Hz and 166 Hz were used for testing to obtain the optimal anodized oxide layer. As shown in Fig. 1(a, b), an anodized oxide layer was locally formed on the surface when a current of 100 mA/cm^2 was applied. On the other hand, a rougher and more heterogeneous oxide layer was observed when a current of 200 mA/cm^2 was applied, as shown in Fig. 1(c, d). Fig. 1(c) shows the results where 50 Hz of pulse was applied. Meanwhile, partly oxide layer was formed when a pulse of 166 Hz was applied 200 mA/cm^2 as shown in Fig.1 (d). In Fig. 1(e, f), where a current of 300 mA/cm^2 was applied, a thick and heterogeneous oxide layer was formed over the entire surface. In Fig. 1(e) where a pulse of 50 Hz was applied, homogenized pores with a pore size of approximately 20–60 μm were observed. In Fig. 1(f), where a pulse of 166 Hz was applied, the oxide layer with a rough surface was formed and overgrown. In a previous study, when the same electrolytic solution used in this study was applied to an AZ91D alloy, the anodized layer with the most homogenous porosity was formed under the following conditions: a current density of 300 mA/cm^2 , 125 Hz, and 3 minute treatment [12].

Nevertheless, a current density of 100–300 mA/cm^2 and frequency of 50 Hz and 166 Hz were applied again as the composition of the alloy used was different. As a result of anodization, the most appropriate oxide layer was obtained in Mg-35Zn-3Ca under a current density of 300 mA/cm^2 and a frequency of 50 Hz (Fig. 1(e)). In the cases of the groups treated with a current density of 100 mA/cm^2 , it was difficult to obtain the formation of a complete oxide layer within the treatment time regardless of the frequency applied.

Fig. 2 shows a cross section SEM image of the samples shown in Fig. 1. The increase in frequency and pulse current

enabled the acquisition of a regular and compact film compared with the sample group having an irregular cross section when DC was used. The film thickness formed at $100\text{--}200\text{ mA/cm}^2$ (Fig. 2(a-d)), ranged from $8\text{--}20\text{ }\mu\text{m}$, but the film thickness formed over 200 mA/cm^2 (Fig. 2(e,f)) was $35\text{ }\mu\text{m}$, suggesting a thicker film forms at higher current and frequency. In the cross sectional analysis result, the separation between the substrate and the film was barely observable as the frequency was increased. This is beneficial to the strength of the formed film and to the binding force with the substrate.

Fig. 3 and Table III shows the surface roughness of the six groups treated with various currents and frequencies. R_a was shown to increase with increasing current but there was no difference in roughness due to the change in frequency. On the other hand, in Fig. 3(E), where 300 mA/cm^2 and 50 Hz were applied, R_a was $1.185\pm 0.232\text{ }\mu\text{m}$, which was the lowest among formed complete oxide film (Fig. 3(C-F)), where the entire surface was covered with the oxide layer, which also had low R_y as $8.767\pm 1.278\text{ }\mu\text{m}$. When a current density of 300 mA/cm^2 and a frequency 50 Hz were applied, the lowest R_a and R_y were obtained in the oxide layer. Therefore, the oxide layer is likely to be maintained stably under the aforementioned condition. The excessive formation of oxide layers builds a double layer on top of the layer already formed, and is detached easily due to cracks and overgrowth as the spark increases [13].

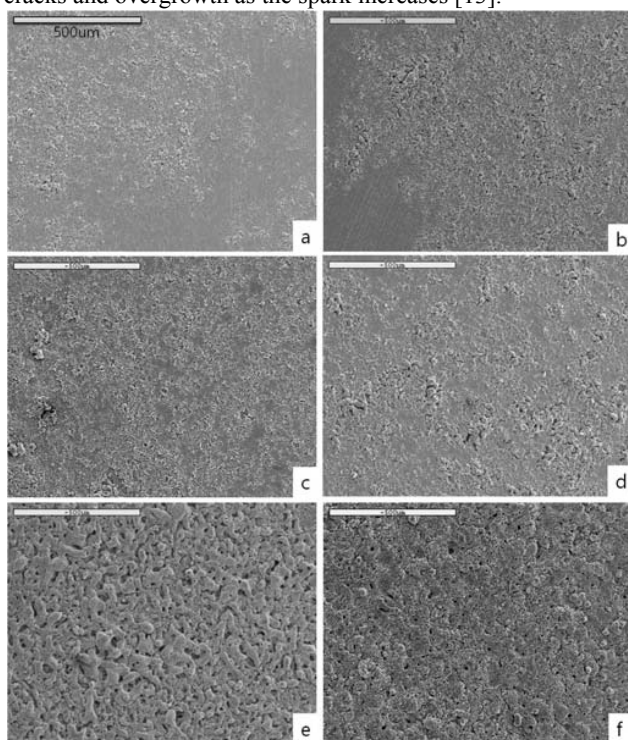


Fig. 1 Surface morphology of Mg-35Zn-3Ca alloy after anodization, applied (a) current 100 mA/cm^2 , frequency 50 Hz , (b) current 100 mA/cm^2 , frequency 166 Hz , (c) current 200 mA/cm^2 , frequency 50 Hz , (d) current 200 mA/cm^2 , frequency 166 Hz , (e) current 300 mA/cm^2 , frequency 50 Hz , (f) current 300 mA/cm^2 , frequency 166 Hz .

Fig.4 shows the result of potentiodynamic polarization for corrosion assessment. The potential voltage is -1.53 V in the untreated Mg alloy (Fig.4 (a)) and highest potential voltage -0.806 V in the anodized group by high current (Fig.4 (g)). The corrosion voltage increases, which resulted in an improvement of the corrosion resistance after surface treatment. When potentiodynamic polarization was conducted of treated 300 mA/cm^2 (Fig.4(f and g)), both groups have similar potential voltage value but current density of treated 300 mA/cm^2 , frequency 166 Hz (Fig.4(g)) has lower than Fig.4(f). For good corrosion resistance, the result should be low current density and high potential voltage, generally. The surface corrosion resistance of Mg and Mg alloy can particularly achieve the maximum effect through anodization [14]. MC3T3-E1 cells ($2.5 \times 10^4\text{ cells ml}^{-1}$) was stained with 0.3% crystal violet, and observed by optical microscopy in Fig.5. MC3T3-E1 cells are osteoblast cells isolated from the skulls of neonatal rats. They initially look like fibroblasts, and show high activity after long-term culture. In addition, they differentiate into osteoblast and bone cells, and cause calcification of the bone matrix [15]. Compared to the negative group (Fig.5 (h)), the cell bioactivity was similar or higher in formed complete oxide film (Fig. 5(e-g)), but the cell viability show low in uncompleted groups as (Fig. 5(a-d)). Uncompleted oxide surface make it local and pitting corrosion, caused by degradable property of Mg alloy by nature.

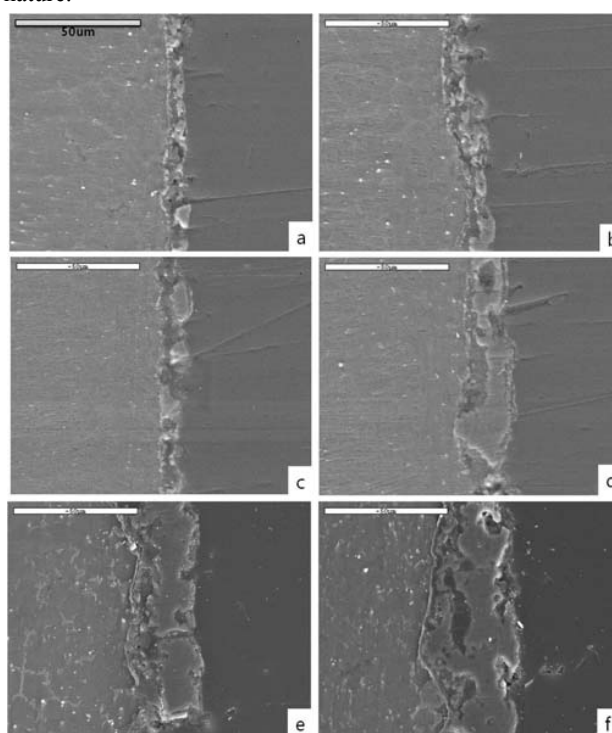


Fig. 2 film thickness of Mg-35Zn-3Ca alloy after anodization (a) current 100 mA/cm^2 , frequency 50 Hz , (b) current 100 mA/cm^2 , frequency 166 Hz , (c) current 200 mA/cm^2 , frequency 50 Hz , (d) current 200 mA/cm^2 , frequency 166 Hz , (e) current 300 mA/cm^2 , frequency 50 Hz , (f) current 300 mA/cm^2 , frequency 166 Hz .

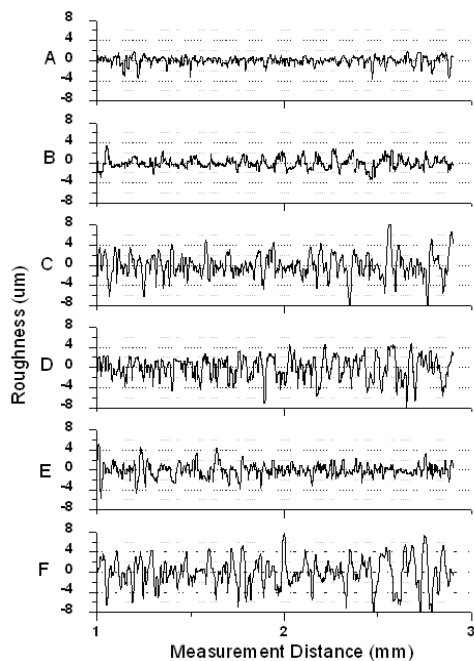


Fig. 3 Change in the roughness with the current density and time of anodization as listed Table III.

TABLE III
VARIATION OF THE ROUGHNESS WITH CURRENT DENSITY AND TIME OF ANODIZATION

Group	Current (mA/cm ²)	Frequency (Hz)	Ra (μm)	Ry (μm)
A	100	50	0.621±0.027	3.318 ±2.378
B	100	166	0.752±0.074	5.807±0.778
C	200	50	1.851±0.197	12.573±1.023
D	200	166	1.643±0.283	9.514±1.785
E	300	50	1.185±0.232	8.767±1.278
F	300	166	2.170±0.212	14.757±0.756

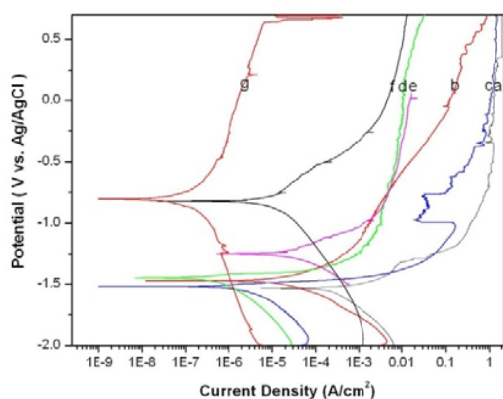


Fig. 4 Potentiodynamic polarization curve (a) untreated Mg-35Zn-3Ca alloy, (b) current 100 mA/cm², frequency 50 Hz, (c) current 100 mA/cm², frequency 166 Hz, (d) current 200 mA/cm², frequency 50 Hz, (e) current 200 mA/cm², frequency 166 Hz, (f) current 300 mA/cm², frequency 50 Hz, (g) current 300 mA/cm², frequency 166 Hz

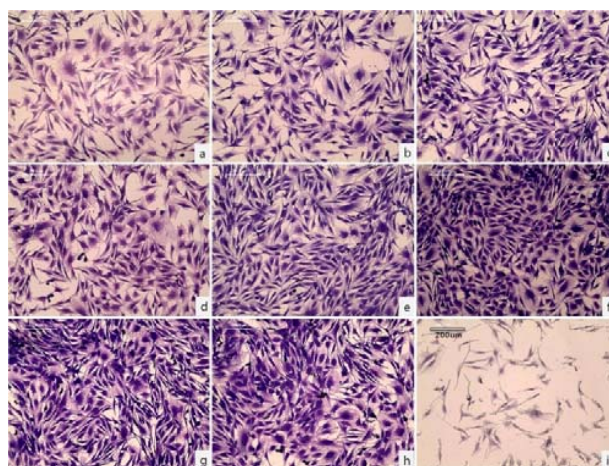


Fig. 5 Optical image of the stain in the marrow cells solution: (a) untreated Mg-35Zn-3Ca alloy, (b) current 100 mA/cm², frequency 50 Hz, (c) current 100 mA/cm², frequency 166 Hz, (d) current 200 mA/cm², frequency 50 Hz, (e) current 200 mA/cm², frequency 166 Hz, (f) current 300 mA/cm², frequency 50 Hz, (g) current 300 mA/cm², frequency 166 Hz, (h) negative, (i) positive

As a result of anodization, the most appropriate oxide layer was obtained in Mg-35Zn-3Ca under a current density of 300 mA/cm² and a frequency of 50 Hz (Fig. 1 (e)). Although the corrosion voltage and mechanical properties of Mg-35Zn-3Ca alloy is lower than commercially available alloys, Al is harmful to the nervous system and osteoblasts [4, 16] and RE metals (Pr, Ce, Y etc.) cause hematotoxicity [17]. Therefore, the biocompatibility of the Mg-35Zn-3Ca alloy is expected to be superior to that of the commercially available alloys, and the improvement in corrosion resistance and mechanical properties is expected to be achieved by post-treatment.

IV. CONCLUSION

The aim of this study is providing protection against corrosion applied micro-arc oxidation by pulse power and current variation on new magnesium alloys (Mg-35Zn-3Ca). After treatment, it was measured of surface properties and biocompatibility. Applying current under 200mA/cm², the oxide film is irregular and incompleteness on surface irrespective of frequency. As a result of potentiodynamic, the corrosion current decreased and the corrosion voltage increased in the high current anodized group. The most appropriate oxide layer was obtained in Mg-35Zn-3Ca under a current density of 300 mA/cm² and a frequency of 50 Hz. Accordingly, in this study, Ca was added to prepare a Mg-35Zn-3Ca alloy for grain refinement, instead of containing Al. In addition, for the improvement of corrosion resistance, pulse anodization was performed in an electrolytic solution containing Si, Ca and P, which assists bioactivity to reform the surface.

ACKNOWLEDGMENT

This work was financially supported by the 'National Research Foundation of Korea (NRF) grant funded by the Korea government (MEST) (No. 2011-0028709)' and 'Basic

Science Research Program through the National Research Foundation of Korea (NRF) funded by the Ministry of Education, Science and Technology (2010-0023901).

REFERENCES

- [1] J. E. Gray and B. Luan, "Protective coatings on magnesium and its alloys — a critical review," *Journal of Alloys and Compounds* vol. 336, pp. 88-113, 2002.
- [2] H. Kuwahara, N. Mazaki, M. Mabuchi, C. Wein, and T. Aizawa, "Behavior of magnesium in Hank's solution aimed to trabecular pattern of natural bone," *Materials Science Forum* vol. 419-422, pp. 1007-1012 2003.
- [3] H. Kuwahara, Y. Al-Abdullat, N. Mazaki, S. Tsutsumi, and T. Aizawa, "Precipitation of Magnesium Apatite on Pure Magnesium Surface during Immersing in Hanks solution," *Materials transactions* vol. 42, pp. 1317-1321 2001.
- [4] H. Li, Y. He, and Z. D. Zeng, "A neural network model for prediction on mechanical properties of QA110-5-5 aluminum bronze after aging," *Jinshu Rechuli/Heat Treatment of Metals*, vol. 31, pp. 28-30, 2006.
- [5] V. T. Truong, P. K. Lai, B. T. Moore, R. F. Muscat, and M. S. Russo, "Corrosion protection of magnesium by electroactive polypyrrole/paint coatings," *Synthetic Metals*, vol. 110, pp. 7-15, 2000.
- [6] A. A. Voevodin, A. L. Yerokhin, V. V. Lyubimov, M. S. Donley, and J. S. Zabinski, "Characterization of wear protective Al-Si-O coatings formed on Al-based alloys by micro-arc discharge treatment " *Surface and Coatings Technology* vol. 86-87, pp. 516-521 1996.
- [7] W. B. Xue, Z. W. Deng, R. Y. Cheng, and T. H. Zhang, "Growth regularity of ceramic coatings formed by microarc oxidation on Al-Cu-Mg alloy " *Thin Solid Films*, vol. 372, p. 114, 2000.
- [8] V. S. Rudnev, T. P. Yarovaya, D. L. Boguta, L. M. Tyrina, P. M. Nedozorov, and P. S. Gordienko, "Anodic spark deposition of P, Me(II) or Me(III) containing coatings on aluminium and titanium alloys in electrolytes with polyphosphate complexes " *Journal of Electroanalytical Chemistry* vol. 497, pp. 150-158 2001.
- [9] A. L. Yerokhin, A. Leyland, and A. Matthews, "Kinetic aspects of aluminium titanate layer formation on titanium alloys by plasma electrolytic oxidation " *Applied Surface Science* vol. 200, pp. 172-184, 2002.
- [10] H. Duan, K. Du, C. Yan, and F. Wang, "Electrochemical corrosion behavior of composite coatings of sealed MAO film on magnesium alloy AZ91D," *Electrochimica Acta*, vol. 51, pp. 2898-2908, 2006.
- [11] (1999). *Biological evaluation of medical devices. Part 5. Tests for cytotoxicity: in vitro methods Arlington, VA: ANSI/AAMI ISO 10993-5.*
- [12] Y. S. Jang, Y. K. Kim, I. S. Park, S. J. Lee, M. H. Lee, J. M. Yoon, and T. S. Bae, "Film characteristics of anodic oxidized AZ91D magnesium alloy by applied power," *Surface interface analysis*, vol. 41, pp. 524-530, 2009.
- [13] I. S. Park, Y. S. Jang, Y. K. Kim, M. H. Lee, J. Yoon, and T. S. Bae, "Surface characteristics of AZ91D alloy anodized with various conditions," *surface and interface analysis*, vol. 40, pp. 1270-1277, 2008.
- [14] I. Ostrovsky, "Method of anodizing of magnesium and producing conductive layers on anodized surface," United states Patent, 2003.
- [15] N. Kurihara, S. Ishizuka, M. Kiyoki, Y. Haketa, K. Ileda, and M. Kumegawa "Effects of 1,25-dihydroxyvitamin D3 on osteoblastic MC3T3-E1 cells," *Endocrinology*, vol. 118, pp. 940-947, 1986.
- [16] S. El-Rahman, "Neuropathology of aluminum toxicity in rats (glutamate and GABA impairment)," *Pharmacological Research*, vol. 47, pp. 189-194, 2003.
- [17] N. Yumiko, T. Yukari, T. Yasuhide, S. Tadashi, and I. Yoshio, "Differences in behavior among the chlorides of seven rare earth elements administered intravenously to rats," *Fundam Appl Toxicol*, vol. 37, pp. 106-116, 1997.